Mineralogical Magazine, October 1998, Vol. 62(5), pp. 647–656

The kinetics of dehydration in Ca-montmorillonite: an *in situ* X-ray diffraction study

HELEN J. BRAY[1], SIMON A. T. REDFERN[1] AND SIMON M. CLARK[2]

[1] Department of Earth Sciences, University of Cambridge, Downing Street, Cambridge, CB2 3EQ, UK
[2]CLRC, Daresbury Laboratory, Daresbury, Warrington, WA4 4AD, UK

ABSTRACT

The thermal dehydration of naturally occurring Ca-montmorillonite has been studied by *in situ* X-ray diffraction at temperatures between 60–120°C. The time-temperature-dependence of the position of the basal (001) reflection reveals that interlayer water loss on isothermal dehydration occurs in two stages. After an initial rapid decrease in interlayer spacing (on shock heating to an isothermal soak temperature) the reaction proceeds towards equilibrium more slowly. Furthermore, the width of the (001) reflection changes with time, reflecting transformation-dependent changes in homogeneity perpendicular to (001) with a maximum in peak width at the point where the rate of the reaction appears to change. This suggests that, as the interlayer spacing collapses, a local change is induced in the structure, affecting the means of movement of the water from the interlayer.

KEYWORDS: montmorillonite, dehydration, synchrotron radiation, smectite, kinetics.

Introduction

SMECTITES found in shale formations during oil and gas exploration are often sources of borehole instability. Maintaining the stability of the well-bore is made difficult because the swelling response of smectites upon contact with aqueous drilling muds of different water activity results in hole enlargement or failure (Hall *et al.*, 1986). In response to this problem, mud additives, such as potassium and polymers, are used to reduce or retard swelling (Steiger, 1982) and to avoid such problems as hydrational stresses.

Koster van Groos and Guggenheim (1989) found that understanding the dehydration of smectites may also be important in predicting their behaviour as they are transported down subduction zones at continental margins. Dehydration in subduction zones has been cited as a potentially important factor in causing shallow focus earthquakes and partial melting in the overlying mantle (Wu *et al.*, 1997). In addition, the dehydration of smectites in sedimentary rocks plays an important role in diagenetic processes (Ransom and Helgeson, 1995). The conversion of smectite to illite in shales, for example, is a proposed mechanism for generating overpressuring in sedimentary basins (Hall *et al.*, 1986). The water expelled from shales may also be important in the primary migration of hydrocarbons (Magara, 1975). Furthermore, smectites form a significant component of raw clay material used in the manufacture of fired ceramics. It is clearly important in all of these applications to understand the response of smectites to changing temperature. This paper presents new experimental results which have shed light on the temperature-time dependence of smectite dehydration.

The 2:1 layer clays consist of negatively charged mica-like sheets which are held together by charge-balancing counterions such as Na^+ and Ca^{2+}. In the presence of water, the counterions hydrate and the interlayer water forces the clay layers apart. The interlayer configuration, and therefore the swelling properties of the clay, is controlled by a number of factors including composition (total layer charge and charge location), interlayer cation (type, valency and hydration energy) and external environment (humidity, temperature and H_2O pressure). Here, the hydration and dehydration of smectites has

been studied using *in situ* techniques in order to quantify the time–temperature-dependent behaviour of these so-called 'swelling clays'.

Early thermal analysis of montmorillonites performed from room temperature to 300°C, pointed to a dehydration reaction below 250°C (Tettenhorst, 1962). This endothermic reaction starts with a quick mass loss at temperatures below 150°C, followed by a slower, more constant mass loss at higher temperatures. The dehydration and rehydration behaviour of these clays has been studied by many workers (Laird *et al.,* 1995; Laird, 1996; Parker, 1986; van Olphen, 1965; Kittrick, 1969a; 1969b). Crystalline swelling occurs in a number of discrete steps, corresponding to the intercalation of zero, one, two, three and four layers of water molecules (Hendricks and Jefferson, 1938; Barshad, 1949; Norrish, 1954). The swelling of the interlayer spans a wide range of d_{001} spacings. In this study the range from 10–15 Å is investigated. Crystalline swelling is believed to be controlled by a number of factors. Attractive forces comprise Coulombic interactions between the interlayer cations and the sites of negative charge on the crystalline layers and van der Waals attraction between the layers. Repulsive forces exist between the like-charged tetrahedral silicate surfaces of the 2:1 layers. Expansion and collapse of the interlayer region may also add elastic terms to the free energy of local strain interactions (often referred to as 'resistance'). Hysteresis, readily seen in this process, is believed to be due to the fact that crystalline swelling is a thermodynamically irreversible process (Laird *et al.,* 1995). Laird (1996) presented a model of the crystalline swelling of 2:1 layer phyllosilicates. His numerical model which comprises a number of potential energies due to attraction, repulsion and elastic terms yields reasonable estimates of basal spacing for octahedrally charged clays.

Koster van Groos and Guggenheim (1984, 1986, 1989), found that montmorillonite dehydrates in two stages. Furthermore, the dehydration reaction does not have a clear end-point and therefore it cannot be analysed straightforwardly by thermogravimetry or other thermal analysis techniques, since it appears that dehydroxylation begins before dehydration is complete. Differential scanning calorimetry (DSC) measurements record the onset of dehydroxylation around 450°C. From isothermal thermogravimetry experiments, montmorillonites typically contain around 10 wt.% water at ambient conditions. This is, however, dependent on relative humidity, temperature, pressure, pH and type of interlayer cation. The removal of interlayer water results in a decrease in the 001 interlayer *d*-spacing. Rehydration of the anhydrous phase eventually becomes impossible when the exchangeable cation itself migrates, either into the crystalline structure, or as it becomes associated with the outer tetrahedral sheets (Greene-Kelly, 1953; Tettenhorst, 1962).

The molecular structure of water and the distribution of counterions in the interlayer region of smectites are the subjects of intense current research (Boek *et al.,* 1995; Chang *et al.,* 1995; Skipper *et al.*, 1989, 1991, 1995*a*; Bridgeman *et al.*, 1996; Karaborni *et al.*, 1996). There remain many questions regarding the role of hydration and the attractive versus repulsive forces at play, as well as those regarding the extent to which specific counterions hydrate the interlamellar space. Molecular dynamics simulations have been performed, and provide new insights at the atomic level. Indeed, computer methods have proved invaluable, since microscopic information from, for example neutron inelastic scattering, is generally inaccessible, since smectites occur in small platelets and disordered powders. Good agreement was found to exist between simulation results (Chang *et al.* 1995; Skipper *et al.*, 1989; 1991, 1995*a*; Bridgeman *et al.*, 1996; Karaborni *et al.*, 1996) and the available experimental diffraction and thermodynamic data (Greene-Kelly, 1955; Low, 1979; Moore and Hower, 1986; Huang *et al.*, 1994; Wu *et al.*, 1997).

The majority of the data obtained from computer simulations have so far focused on samples containing either Na^+ or Mg^{2+} (Bridgeman *et al.,* 1996; Chang *et al.*, 1995; Karaborni *et al.*, 1996; Skipper *et al.*, 1989, 1991, 1995*a,b*). Molecular dynamics and Monte Carlo simulations show that three hydration states exist related to 'one-', 'two-' and 'three-layer' hydrates, where the layers correspond to semi-ordered H_2O structures. These simulations have indicated that the interlayer H_2O structure deviates significantly from the structure of bulk liquid water, being significantly structurally correlated, with the development of a less organized structure with increasing interlayer water content and layer separation. The spatial distribution of the exchangeable cations varies with the degree of hydration, and the extent of charge deficiency at the surface of the alumino-

silicate layer (the structural charge). Negative charge associated with Al^{3+} substituting for Si^{4+} in the tetrahedral layer should be localized on the three surface oxygens attached to the Al^{3+}, whereas the charge associated with substitution in the octahedral layer (Mg^{2+}or Fe^{2+} for Al^{3+}) is more diffusely spread over the surface oxygens (Farmer and Russell, 1967).

Whilst significant progress has been made by computer simulation methods, there remains little *in situ* structural crystallographic information on the dynamics of either hydration or dehydration at high temperature. A recent study by Wu *et al.* (1997) has shown that synchrotron radiation may be used to observe equilibrium hydration states of montmorillonite at high temperatures and pressures, although they do not report results for the time-dependence of either dehydration or rehydration. Understanding the kinetics of water mobility in this structure, however, is essential in many industrial applications, especially in the ceramics industry. Here, therefore, we have used synchrotron radiation to probe the time-temperature dependence of hydration-related structural rearrangements in Ca-montmorillonite, using synchrotron X-rays.

Synchrotron radiation sources provide intense beams of high-energy X-ray photons with characteristics that can be exploited in the study of fast reaction kinetics within bulk solid state materials, as has recently been shown for the kaolinites (Bellato *et al.,* 1995) and the hydration of cements (Barnes *et al.*, 1996). Here, the dehydration reactions of smectite have been followed by dynamic high temperature energy dispersive diffraction (EDD) using synchrotron radiation, at the Daresbury synchrotron radiation source, where spectra can be collected every three seconds. This allows the rapid reaction kinetics of early stage dehydration to be followed dynamically *in situ* by a structural crystallographic probe.

Experimental

The sample studied was a naturally occurring Ca-montmorillonite from Redhill, Surrey, England sold by Redland Minerals, kindly provided by Dr S Drachman of Redland Braas Building R & D. Analysis of the sample showed a smectite-rich clay (98.0% smectite, 0.5% kaolinite, 1.0% quartz for whole-rock analysis by X-ray diffraction). The sample was initially ground by hand with a pestle and mortar and dry sieved below 53 μm.

The dehydration of montmorillonite has been followed by time-resolved energy dispersive (ED) synchrotron experiments, performed at CLRC Daresbury laboratory on station 16.4 of the six Tesla Wiggler beam line. The experimental set-up, described in detail by Clark (1996), employs white radiation passing through the sample, and an energy-dispersive solid-state detector held at a fixed scattering angle (in this experiment $2\theta = 1°$). The scattering angle was calibrated at the end of the set of experiments against the d_{001} for pyrophyllite.

Around 30 mg of sample was loosely packed into a pyrophyllite disk sample holder. The furnace used was a modified Linkam 1500 microscope furnace, with the sample disk placed at the center of the heating element. A pure argon purge flowed through the sample chamber to drive away any evolved water. Constant heating rate experiments from room temperature up to 1200°C at various heating rates (10, 25, 50, 75 and 99°C/min), and isothermal dehydration experiments were performed by shock heating the sample to the desired temperature (between 60 and 120°C) and then holding the temperature constant for two hours.

In ED powder diffraction, a polychromatic 'white' X-ray beam passes through the sample and forward-scattered Bragg reflections are intercepted by an energy dispersive germanium detector at a small fixed scattering angle. The Bragg condition, expressed familiarly as $2d\sin\theta = n\lambda$ for wavelength dispersive diffraction, becomes $Ed\ \sin\theta = 6.199$ keV for energy-dispersive, where E is the photon energy in keV, d the lattice spacing in Å and 2θ the scattering angle in degrees. The sample is positioned at the lozenge of intersection of the collimated incoming X-ray beam and the collimated diffracted beam. The diffracted beam impinges upon the energy dispersive detector, which in turn feeds into a 4000 channel multichannel analyser.

The data acquisition times varied between 3 and 14 seconds (depending on the temperature cycle imposed), chosen to maintain a good signal to noise ratio. Two sets of experiments were performed. In the first runs, diffraction patterns were collected under constant heating rate in order to provide a preliminary assessment of the reaction kinetics. Different values of heating rates were used (10, 25, 50, 75, and 99°C/min) over a temperature range of 25 to 1200°C. In addition, isothermal experiments were performed at 60, 70, 80, 90, 100, 110, and 120°C. They provide a more

detailed insight into the reaction occurring on the atomic scale, as well as revealing the behaviour of the interlayer of water, as a function of temperature, and the variation in homogeneity of its structural state with time.

The evolution of the reaction was followed by the change in the spacing given by the basal reflection. Since the stacking of the crystalline layers is irregular along the x and y crystallographic axes, the (001) peak is the only significant reflection collected at this low scattering angle. The position and width of the (001) reflection can be determined by fitting the profiles to a Gaussian function. The change in position and width of this reflection indicate the loss of water and the spatial heterogeneity (i.e. distribution of local interplanar spacings) of the process, respectively.

Results and discussion

The profiles seen in Figs 1*a* and *b*, show a decrease in the basal spacing of montmorillonite with time and temperature. As temperature increases, asymmetric peak broadening and a decrease of intensity of the (001) reflection are also observed. Diffuse scattering is apparent at large d-spacings and may be due to interference effects between crystal interfaces, reflecting the small particle size.

Initial (t_o) values of interplanar spacings for Ca-montmorillonite differ from run to run (Figs. 1*a,b* and 2). This is due to a small variation of water content in the interlayer region at the start of the heating experiment. This variation arose from variable time lags between putting the sample in the dry Ar gas flow and starting the data collection. This is in itself an unavoidable feature of our experimental arrangement, since the use of synchrotron radiation necessitates operating hutch interlocks, shutter delay, remote operations and other safety features which impose the time lag between starting the gas flow and starting a temperature cycle. In constant heating rate runs, there is a slight decrease in the rate of dehydration when the sample reaches a bulk water content equivalent to a d_{001} spacing of around 12.5 Å (Fig. 2). A loss of intensity of the 001 reflection is observed after the sample has attained an interlayer configuration of 10.3 Å. At slower heating rates, the 001 peak disappears entirely at around 300°C. The disappearance of the 001 reflection on dehydration is due to the breakdown in periodicity parallel to z^*, associated with the

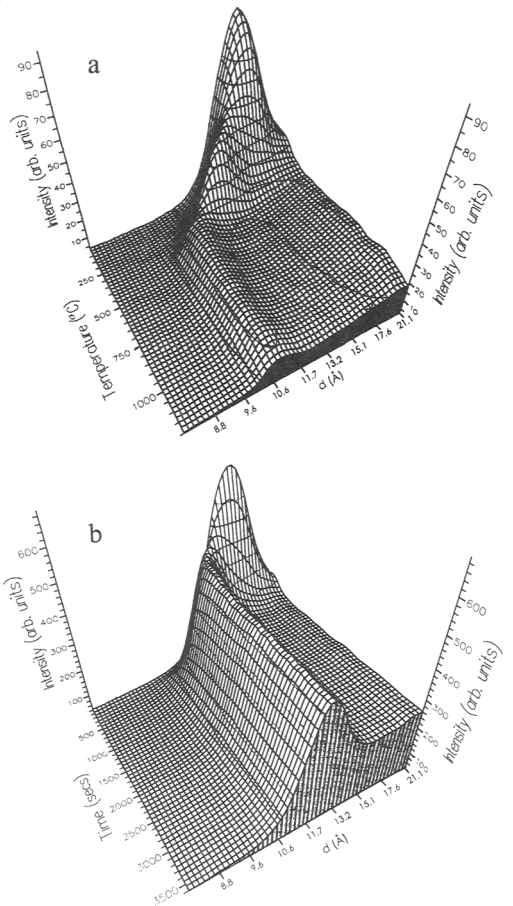

FIG. 1. (*a*) Energy-dispersive X-ray diffraction patterns of Ca-montmorillonite as a function of temperature, collected during the 75°C/min rising temperature experiment, showing a decrease in basal spacing. (b) Time-dependence of the (001) reflection of Ca-montmorillonite during the isothermal experiment at 60°C (spectra collected every 14 seconds for 2 hours).

random interstratification and concomitant randomly distributed local strains in the 2:1 layers.

The formation of new phases at higher temperatures (such as mullite and other refractory phases) is not observed due to the low fixed scattering angle used. From the data it is apparent that the '11.7 Å' and '10.3 Å' states could be considered as locally stable phases, the steeper $d(d_{001})/dT$ regions representing more rapid kinetically controlled structural response (as water loss) during heating.

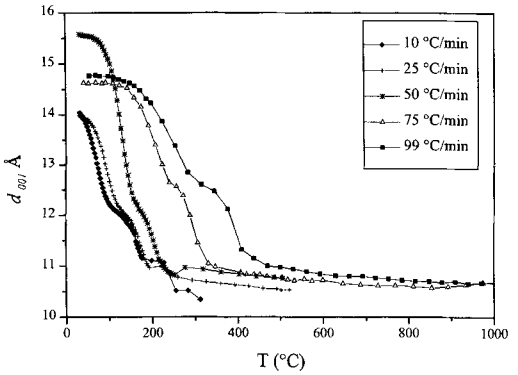

FIG. 2. Decrease in basal spacing with increasing temperature for different heating rate runs, determined from synchrotron X-ray diffraction.

Isothermal high-temperature experiments (Fig. 3) show a decrease in basal spacing with time in a similar manner to the constant heating rate experiments. At 100°C a large and rapid change in d_{001} occurs in the first 500 seconds, leaving the reaction to then proceed at a slower rate (Fig. 3*a*). A control experiment, at identical soak temperature (T), where no gas flow was employed, showed similar behaviour. The full width at half maximum (FWHM) of the 001 peak increases to a maximum coincident with the inflection point of the rapid decrease in basal spacing, during the first part isothermal dehydration. The change in FWHM represents a change in spatial heterogeneity of the sample and it can be inferred that a wide range of interplanar spacings are present (Fig. 3*b*). The sudden change in heterogeneity of the sample during the initial shock heating and relaxation towards equilibrium is a common feature of metastable behaviour in minerals (Salje, 1990). The interlayer region appears to be dehydrating at two different rates dependent on reaction coordinate as the more stable configuration is approached. We note that even the experiments run for the longest times do not appear to have reached a constant d-spacing, although the approach to a stable interlayer spacing can only be expected to be asymptotic in such an experiment.

The reaction appears complex, as can be seen from the change in FWHM (Fig. 3*a*). Following the work of Miletich *et al.* (1997), we have used an exponential decay to calculate the time dependence of d_{001}, and hence the end-point of dehydration at each temperature. The data from t > 1000 secs onwards were fitted by a least squares procedure to a simple exponential function:

$$d(001)_0 = d(001)_\infty + \Delta d e^{-\{k(t - t_0)\}n} \quad (1)$$

where $d(001)_0$ is the initial d-spacing, $d(001)_\infty$ is the value at $t = \infty$, and $\Delta d = d(001)_0 - d(001)_\infty$. The reaction coordinate at a specific temperature can now be calculated for $d(001)$ at time t:

$$\frac{d(001)_t - d(001)_\infty}{d(001)_0 - d(001)_\infty} \quad (2)$$

The data resulting from these fitting procedures are shown in Fig. 4, where the values of $d(001)_\infty$ from this fitting procedure are compared to the experimentally determined ones for the longest time duration of the experiments (t = 3600 secs). The equilibrium basal spacing can be determined as a function of temperature from the calculated

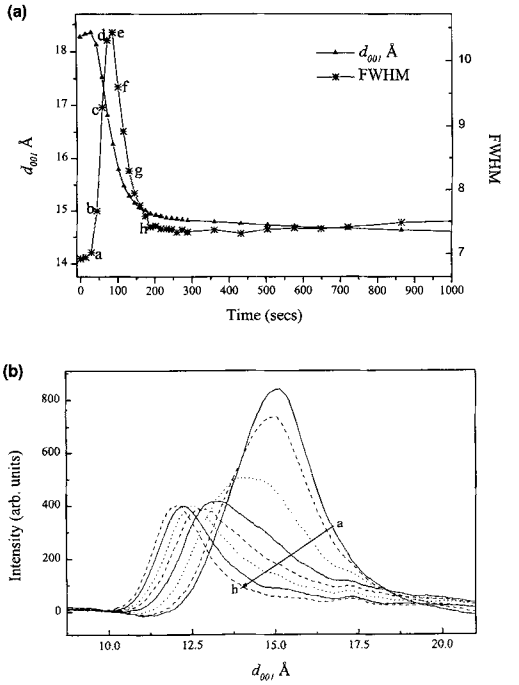

FIG. 3. (*a*) Time-dependence of the full width at half maximum (FWHM) and d-spacings of the (001) reflection, during the 100°C isothermal experiment. (*b*) Variation in the (001) reflections on heating, shown as a function of reaction, progressing from (a) to (h). The peak profiles change from a symmetric peak shape to an asymmetrically broadened one, before returning to a narrower symmetric shape.

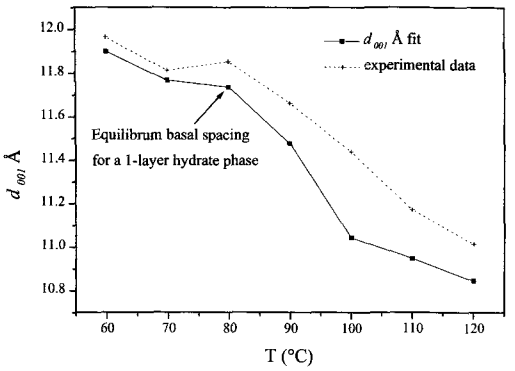

FIG. 4. Experimental and calculated d-spacings after long isothermal heating runs compared with those calculated at infinte time, as a function of temperature. Data have been fitted to the simple exponential function given in Equation 3.

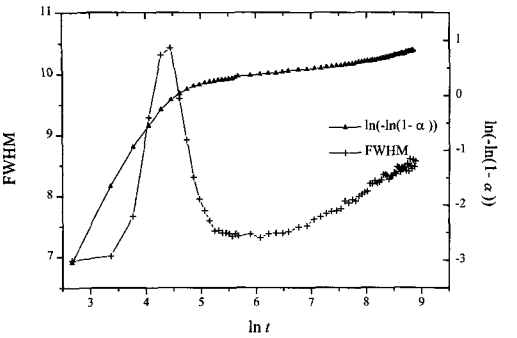

FIG. 5. Plot, showing the change in FWHM of the (001) reflection, and the simultaneous change in gradient of $\ln(-\ln(1-\alpha))$ related to a change in rate controlling reaction mechanism.

basal spacings between 60–120°C (Fig. 4). The results proved valuable as a basal spacing of 11.7 Å can be attributed to a one-layer hydrate. This value of d_{001} is the same as that at which there is a decrease in rate of dehydration observed in the non-isothermal results.

Clay minerals are heterogeneous systems and the reaction followed by the isothermal experiments appears complex from the change in FWHM. It is found that the isothermal kinetics of a reaction can be described empirically by the equation:

$$\frac{dy}{dt} = k^n t^{n-1}(1-\alpha) \qquad (3)$$

where k is a rate constant of the reaction, t is the time and α is the fraction transformed. The variable n is a constant that depends on reaction mechanism, n greater than 1 implies a phase boundary controlled reaction and, n less then 1 indicates a diffusional process. Upon integration of equation (3), the fraction transformed can be written as the Avrami equation:

$$-\ln(1-\alpha) = (kt)^m \qquad (4)$$

which can be re-expressed in linearised form as:

$$\ln(-\ln(1-\alpha)) = m\ln k + m\ln t \qquad (5)$$

A 'lnln' plot allows one to determine a value for both reaction mechanism (m) and the rate constant (k). This process has been applied to our diffraction data. Deviations from linearity show that the data deviate from the expected Avrami equation (Fig. 5) for a single reaction mechanism, and indicate the existence of two rate-controlling processes. The value of m from the gradient of the 'lnln' plot can be related to specific rate laws (Hancock and Sharp, 1972). For each isothermal run, a change in gradient through the reaction is believed to be due to a change in controlling reaction mechanism. Therefore the gradient has been measured before and after this change in gradient. The values in Table 1 show that an average value of 0.93 can be inferred for the first stage of dehydration on initial shock heating. This corresponds to the value expected for a first order reaction. However, the gradient varies between datasets, so that a number of phase-boundary kinetic rate equations could almost equally well be selected. Four reaction mechanisms can be considered (indicated by the results in Table 1): a zero-order reaction (zero: $\alpha = kt$), a first-order

TABLE 1. Calculated m values for the initial dehydration reaction, r indicates the coorelation factor for the fit

T °C	m	r
120	1.14	0.993
110	1.02	0.995
100	0.82	0.987
90	0.85	0.991
80	1.00	0.996
70	0.77	0.999
60	0.94	0.997

reaction (F1 [$-\ln(1 - \alpha) = kt$]), or a phase-boundary-controlled mechanism with either cylindrical (R2: [$1 - (1 - \alpha)^{1/2} = kt$]) or spherical symmetry (R3: [$1 - (1 - \alpha)^{1/3} = kt$]).

Considering the structure of Ca-montmorillonite, a phase-boundary-controlled reaction might be expected if the collapse of the interlayer is the rate-controlling factor. The movement of the dehydration front perpendicular to (001) within crystalline layers is indicated by a rapid decrease in basal spacing. Therefore, the initial stage of dehydration could be understood physically in terms of a two-dimensional phase-boundary-controlled reaction (R2) model.

As the reaction proceeds (and the end-point is approached more closely) the reaction rate (and mechanism) appears to change. This second stage of dehydration, linked to slow decrease in basal spacing, has been analysed in the same way and the values of m obtained are presented in Table 2. The average value of m is 0.18, which again does not relate to a specific rate law, but indicates that a two-dimensional diffusion controlled process is probably dominating the movement of water from the collapsed interlayer out to the edges.

Conclusions

Our observed basal spacings of 15, 11.7 and 10.3 Å can be related to two-, one- and zero-layers of water residing in the interlayers of Ca-montmorillonite, respectively (Skipper *et al.*, 1989, 1991, 1995*a,b*). Hall *et al.* (1986) also studied montmorillonite at pressures experienced during the first kilometre of burial and compaction and found that these conditions were sufficient to remove all but the last two interlamellar water sheets from montmorillonite. From the analysis of our data collected at constant heating rates with and without the Ar purge we conclude that water in the second-layer hydrate appears to be held relatively loosely within the interlayer. The last layer of water corresponds to a d_{001} of around 11.7 Å. This is more thermally stable, and dehydration at intermediate temperatures slows down on reaching this configuration (Fig. 4). Krittrick (1969) found similar results on studying a suite of cation-exchanged montmorillonites. He investigated the dehydration/hydration characteristics as a function of hydration energy and charge of the exchangeable cation. The water driven off at more advanced stages of dehydration is more firmly held, believed to be involved in water-cation interactions (Skipper *et al.*, 1989, 1991, 1995*a,b*).

TABLE 2. Calculated m for the second stage of interlayer water dehydration, r indicates the coorelation factor for the fit

T °C	m	r
120	0.23	0.996
110	0.20	0.986
100	0.14	0.989
90	0.14	0.990
80	0.11	0.990
70	0.21	0.984
60	0.25	0.993

The end of dehydration is marked by the breakdown of the interlayer after reaching a d-spacing of 10.3 Å. After dehydration, migration of the exchangeable cations begins, and they become associated with the outer tetrahedral sheet (in the case of Ca) or enter vacant octahedral sites (in the case of Mg) (Hofman and Klemen, 1950; Greene-Kelly, 1955; Farmer and Russell, 1967; Calvet and Prost, 1971). Few studies have been conducted on larger particle fractions of naturally occurring clays. It is not clear whether dehydration is complete before the onset of dehydroxylation, as the very low fixed scattering angle of our experiment and the irregularity in stacking of the layers means that only the fundamental basal spacing was monitored.

All previous kinetic studies on the dehydration of Ca-montmorillonite and other cation-exchanged samples have assumed that the kinetics of dehydration can be described by a single activation energy, remaining constant throughout the transition (e.g. Girgis *et al.*, 1987; Guindy *et al.*, 1985). Difficulties arise, however due to the mechanism of the later stages of the reaction differing from that followed initially, depicted by the change in gradient, $d(d_{001})/dt$, and FWHM of the 001 reflection (Fig. 5) at fairly short times in isothermal experiments. In our experiments, after the initial rapid decrease of the interlayer spacing, the reaction rate decreases. This appears to reflect a change in reaction from a phase-boundary rate determining step to one which is diffusion controlled. Therefore, as the layers collapse, inducing a change in the structure, the means of movement of water from the interlayer spacing is affected. The initial rate of reaction appears

controlled by the collapse of the crystalline layers, but on approaching the final stages it becomes controlled by the diffusion of the water molecules from the interlayer region.

Similar results from the work of Craido *et al.* (1984) on kaolinite and Ruan and Gilkes (1996) on goethite, also indicate that the controlling process changes with temperature, and with fraction transformed (α) in these materials. Ruan and Gilkes (1996), investigating aluminous goethites, found up to three different reaction mechanisms in a single isothermal experiment. In addition, Craido *et al.* (1984) found that in the latter stages of reaction ($\alpha \leqslant 0.6$) the rate limiting mechanism changed from a first-order mechanism to a diffusion controlled reaction. This could explain the differences found between earlier thermal examinations of kaolinite, where the question whether a diffusion-controlled, first-order reaction dominated, was left unanswered (Murray and White, 1955; Allison, 1954; Brindley *et al.*, 1967).

The presence of two controlling reaction mechanisms must be manifested in a change in the dehydration behaviour of the Ca-montmorillonite. The physical significance of the applied kinetic rate laws has been inferred, but a relationship between reaction mechanism and non-equilibrium microstructure can be postulated (Salje and Wruck, 1988). Clay systems are very complicated and can never be treated as homogeneous systems, however, under certain conditions they are less heterogeneous than under others. Initially, at the start of the isothermal shock heating experiments, the material has not begun to dehydrate: a sharp diffraction peak is recorded. This indicates little variation in *d*-spacing throughout the sample, suggesting relatively high structural correlations parallel to z^*. In the response to shock isothermal heating, the basal peak becomes asymmetric (Fig. 3*a,b*), and the peak width diverges to a maximum (Fig. 5). The rate of dehydration during this initial stage is rapid and the system is very far from equilibrium. The distribution of water molecules parallel to z^* is heterogeneous and the removal of water appears controlled by strain effects and the collapse of the interlayer. As the rate of reaction slows down, it becomes diffusion-controlled and the system approaches its final state. A change in reaction mechanism occurs, therefore, and in the later stages of dehydration the profiles sharpen: the system becomes less heterogeneous once more.

Acknowledgements

The authors are grateful to Redland Braas Building R & D for providing CASE studentship funding and to Dr Simon Drachman for his help in his capacity as industrial supervisor. Helpful critical reviews were provided from Drs William Bassett, David Laird and Neil Skipper. This work was supported through NERC grants GT19/95/CS/2 and GR9/03138.

References

Allison, E.B. (1954) Determination of specific heats and heats of reaction of clay minerals by thermal analysis. *Silicates Ind.*, **19**, 363–73.

Barshad, I. (1949) The nature of lattice expansion and its relation to the hydration in montmorillonite and vermiculite. *Amer. Mineral.*, **34**, 675–84.

Barnes, P., Turillas, X., Jupe, A.C., Colston, S.L., David, O., Cernik, R.J., Livesey, P., Hall, C., Bates, D. and Dennis, R. (1996) Applied crystallography solution to problems in solid-state chemistry case examples with ceramics, cements and zeolites. *J. Chem. Soc. Faraday. Trans.*, **92**, 2187–96.

Bellotto, M., Gualtieri, A., Artoli, G. and Clark, S.M. (1995) Kinetic study of the kaolinite-mullite reaction sequence. Part I. Kaolinite dehydroxylation. *Phys. Chem. Minerals*, **22**, 207–14.

Boek, E.S., Coveney, P.V. and Skipper, N.T. (1995) Monte Carlo molecular studies of hydrated Li-, Na- and K- smectites: understanding the role of potassium as a clay swelling inhibitor. *J. Amer. Chem. Soc.*, **117**, 12608–17.

Bridgeman, C.H., Buckingham, A.D., Skipper, N.T. and Payne, M.C. (1996) Ab-initio total energy study of uncharged 2:1 clays and their interaction with water. *Mol. Phys.*, **89**, 879–88.

Brindley, G.W., Sharp, J.H., Patterson J.H. and Narahari, B.N. (1967) Kinetics and mechanism of dehydroxylation processesses. 1. Temperature and vapor pressure dependence of dehydroxylation of kaolinite. *Amer. Mineral.*, **52**, 201–11.

Calvet, R. and Prost, R. (1971) Cation migration into empty octahedral sites and surface properties of clays. *Clays Clay Minerals*, **19**, 175–86.

Chang, F.R.C., Skipper, N.T. and Sposito, G. (1995) Computer simulation of interlayer molecular structure in Sodium montmorillonite hydrates. *Langmuir*, **11**, 2734–41.

Clarke, S.M. (1996) A new energy-dispersive powder diffraction facility at the SRS. *Nucl. Inst. Meth. Phys. Res. A*, **381**, 161–8.

Craido, J.M., Ortega, A., Real, C. and Torres de Torres, E. (1984) Re-examination of the kinetics of the

thermal dehydroxylation of kaolinite. *Clay Minerals,* **19,** 653–61.

Farmer, V.C. and Russell, J.D. (1967) IR absorption spectrometry in clay studies. *Clays Clay Minerals,* **15,** 121–42.

Girgis, B.S., El-Barawy, K.A. and Feli, N.S. (1986) Dehydration kinetics of some smectites: a thermogravimetric study. *Thermochimica Acta,* **98,** 181–9.

Greene-Kelly, R. (1955) Dehydration of montmorillonite minerals. *Clay Minerals Bull.,* **5,** 604–15.

Guindy, N.M., El-Akkad, T.M., Flex, N.S., El-Massry, S.R. and Nashed, S. (1985) Thermal dehydration of mono- and di-valent montmorillonite cationic derivatives. *Thermochimica Acta,* **85,** 211–4.

Hall, P.L., Astill, D.M. and McConnell, J.D.C. (1986) Thermodynamic and structural aspects of the dehydration of smectites in sedimentary rocks. *Clay Minerals,* **21,** 633–48.

Hancock, J.D. and Sharp, J.H. (1972) Method of comparing solid-state kinetic data and its application to the decomposition of kaolinite, brucite and $BaCO_3$. *J. Amer. Ceram. Soc.,* **55,** 74–7.

Hendricks, S.B. and Jefferson, M.E. (1938) Structures of kaolin and talc-pyrophyllite hydrates and their bearing on water sorption of the clays. *Amer. Mineral.,* **23,** 863–75.

Hofman, H. and Klemen, R. (1950) Verlust der Austauschfahigheit von Lithiuimionen an Bentonit durch Erhitzung. *Zeits. Anorg. Chem.,* **262,** 95–9.

Huang, W.L., Bassett, W.A. and Wu, T.C. (1994) Dehydration and hydration of montmorillonite at elevated temperatures and pressures monitored using synchrotron radiation. *Amer. Mineral.,* **79,** 683–91.

Karaboni, S., Smit, B., Urah, J. and van Oort, E. (1996) The swelling of clays: molecular simulations of the hydration of montmorillonite. *Science,* **271,** 1102–4.

Kittrick, J.A. (1969a) Interlayer forces in montmorillonite and vermiculite. *Soil. Sci. Soc. Amer. Proc.,* **33,** 217–22.

Kittrick, J.A. (1969b) Quantitative evaluation of the strong-force model for expansion and contraction of vermiculite. *Soil. Sci. Soc. Amer. Proc.,* **33,** 222–5.

Koster van Gross, A F. and Guggenheim, S. (1984) The effect of pressure on the dehydration reaction of interlayer water in Na-montmorillonite (Swy-1). *Amer. Mineral.,* **69,** 872–9.

Koster van Groos, A.F. and Guggenheim, S. (1986) Dehydration of K-exchanged montmorillonite at elevated temperatures and pressures. *Clays Clay Minerals,* **34,** 281–6.

Koster van Groos, A.F. and Guggenheim, S. (1989) Dehydroxylation of Ca- and Mg-exchanged montmorillonite. *Amer. Mineral.,* **74,** 627–36.

Laird, D.A. (1996) Model for the crystalline swelling of 2:1 layer phyllosilicates. *Clays Clay Minerals,* **44,** 553–9.

Laird, D.A. Shang, C. and Thompson, M.L. (1995) Hysteresis in crystalline swelling of smectites. *J. Coll. Interface Sci.,* **171,** 240–5.

Low, P.F. (1979) Nature and properties of water in montmorillonite-water systems. *Soil. Sci. Amer. J.,* **45,** 651–8.

Magara, K. (1964) Reevaluation of montmorillonite dehydration as cause of abnormal pressure and hydrocarbon migration. *Amer. Assoc. Petroleom. Geol. Bull.,* **59,** 202–9.

Miletich, R., Zemann, J. and Nowak, M. (1997) Reversible hydration in synthetic mixite $BiCu_6(OH)_6(AsO_4)_3.nH_2O$ (n3): hydration kinetics and crystal chemistry. *Phys. Chem. Minerals,* **24,** 411–22.

Moore, D.M. and Hower, J. (1986) Ordered interstratification of dehydrated and hydrated Na-smectite. *Clays Clay Minerals,* **34,** 379–84.

Murray, P. and White, J. (1955) Kinetics of thermal dehydration characteristics of the clay minerals. *Trans. Brit. Ceram. Soc.,* **54,** 137–50.

Norrish, K. (1954) The swelling of montmorillonite. Discuss. *Faraday Soc.,* **18,** 120–34.

Parker, J.C. (1986) Hydrostatics of water in porous media. In *Soil Physical Chemistry* (D.L. Sparks, ed.). Boca Raton, FL: CRC Press. 209–96.

Ransom, B. and Helgeson, H.C. (1995) A chemical and thermodynamic model of dioctahedral 2:1 layer clay minerals in diagenetic processes: dehydration of dioctahedral aluminous smectite as a function of temperature and depth in sedimentary basins. *Amer. J. Sci.,* **295,** 245–81.

Redfern, S.A.T. (1987) The kinetics of dehydroxylation of kaolinite. *Clay Minerals,* **22,** 447–56.

Ruan, H.D. and Gilkes, R.J. (1996) Kinetics of thermal dehydroxylation of aluminous goethite. *J. Therm. Anal.,* **46,** 1223–38.

Salje, E.K.H. (1986) *Phase Transitions in Ferroelastic and Co-elastic Crystals.* Cambridge University Press, Cambridge 202–11.

Salje, E.K.H. and Wruck, B. (1988) Kinetic rate laws as derived from order parameter theory. II Interpretation of experimental data by Laplace-transformation, the relaxation spectra and the kinetic gradient coupling between two order parameters. *Phys. Chem. Minerals,* **16,** 140–7.

Skipper, N.T., Refson, K. and McConnell, J.D.C. (1989) Computer calculation of water-clay interactions using atomic pair potentials. *Clay Minerals,* **24,** 411–25.

Skipper, N.T., Refson, K. and McConnell, J.D.C. (1991) Computer simulation of interlayer water in 2:1 clays. *J. Chem. Phys.* **91,** 7434–45.

Skipper, N.T., Chang, F.RC. and Sposito, G. (1995a) Monte Carlo simulation of interlayer molecular-structure in swelling clay minerals. 1. Methodology.

Clays Clay Minerals, **43,** 285–93.

Skipper, N.T., Sposito, G. and Chang, F.R.C. (1995b) Monte Carlo simulations of interlayer molecular-structure in swelling clay-minerals. 2. Monolayer hydrates. *Clays Clay Minerals,* **43,** 294–303.

Steiger, R.P. (1982) Fundamentals and use of potassium/polymer drilling fluids to minimize drilling and completion problems associated with hydratable clays. *J. Petrol. Tech.,* **24,** 1661–70.

Tettenhorst, R. (1962) Cation migration in montmorillonite. *Amer. Mineral.,* **47,** 769–73.

van Olphen, H. (1965) Thermodynamics of interlayer adsoprtion of water in clays. *J. Coll. Sci.,* **20,** 822–37.

Wu, T.C., Bassett, W.A., Koster van Groos, A.F. and Guggenheim, S. (1997) Montmorillonite under high H_2O pressures: stability of hydrate phases, rehydration hysteresis and the effect of interlayer cation. *Amer. Mineral.,* **82,** 69–78.

[*Manuscript received 2 May 1998*]